

## Interacting growth walk: A model for hyperquenched homopolymer glass?

S. L. Narasimhan,<sup>1,\*</sup> P. S. R. Krishna,<sup>1</sup> A. K. Rajarajan,<sup>1</sup> and K. P. N. Murthy<sup>2,†</sup>

<sup>1</sup>*Solid State Physics Division, Bhabha Atomic Research Centre, Mumbai-400 085, India*

<sup>2</sup>*Institut für Festkörperforschung, Forschungszentrum Jülich GmbH, D-52425 Jülich, Germany*

(Received 12 June 2002; published 10 January 2003)

We show that the compact self-avoiding walk configurations, kinetically generated by the recently introduced interacting growth walk (IGW) model, can be considered as members of a canonical ensemble if they are assigned random values of energy. Such a mapping is necessary for studying the thermodynamic behavior of this system. We have presented the specific heat data for the IGW, obtained from extensive simulations on a square lattice; we observe a broad hump in the specific heat above the  $\theta$  point, contrary to expectation.

DOI: 10.1103/PhysRevE.67.011802

PACS number(s): 61.43.Fs, 05.10.Ln, 36.20.Ey, 87.10.+e

Linear polymers in a poor solvent are known [1] to assume globular configurations below a tricritical temperature  $T_\theta$ , called the  $\theta$  point. These globules acquire denser minimum energy configurations at lower temperatures. In the case of random heteropolymers, the “quenched” random interactions between the constituent monomers frustrate the evolution of the globules towards their minimum energy configurations. They are thus forced to freeze into higher energy configurations (local minima). In fact, the heteropolymer globules serve as “toy models” for protein folding phenomenon [2]. It has been shown recently [3] that even homopolymer globules can freeze into glassy states, due to a self-generated disorder brought about by the competing interactions and chain connectivity during the cooling process. In this sense, the freezing of a homopolymer globule is said to be analogous to that of a structural glass.

In a Monte Carlo study of this freezing process, we may choose a configuration from a canonical ensemble of interacting self-avoiding walks (ISAW) [4] which represents a linear polymer in equilibrium with a thermal bath at a temperature  $T$  (say,  $\geq T_\theta$ ). Then, using a standard dynamical algorithm [5], we may relax the chosen configuration at a temperature preset (i.e., quenched) to a desired value less than  $T_\theta$ ; deeper the quench, more difficult and time consuming it would be to realize a globular configuration. On the other hand, the interacting growth walk (IGW) [6] is a simpler but more efficient algorithm for generating compact or globular self-avoiding walks (SAW); they are generated, step by step, by sampling the locally available sites with appropriate Boltzmann factors,  $\exp(\beta_G n_{NN}^m \epsilon_0)$ , where  $\beta_G^{-1}$  is the “growth” temperature,  $n_{NN}^m$  ( $1 \leq m \leq z-1$ ) is the number of nonbonded nearest neighbor (NBNN) contacts the site  $m$  will make, if chosen, on a lattice of coordination number  $z$  and  $-\epsilon_0$  is the attractive energy associated with any NBNN contact.

In this paper, we show that these kinetically generated IGWs represent the frozen configurations of a homopolymer

globule with a self-generated disorder. Contrary to expectation, our simulations on a square lattice indicate an excess specific heat, characterizing these frozen states, above the  $\theta$  point. In fact, this simple model demonstrates that a meaningful statistical mechanical description of an irreversible growth process involves an element of self-generated disorder brought about by ergodicity breaking of the system.

The growth of an IGW starts by first “occupying” an arbitrarily chosen site  $\mathbf{r}_0$  of a regular  $d$ -dimensional lattice of coordination number  $z$  whose sites are initially “unoccupied” (by monomers). The first step of the walk is taken in one of the  $z$  available directions by choosing an unoccupied nearest neighbors (NN) of  $\mathbf{r}_0$ , say  $\mathbf{r}_1$ , at random and with equal probability. Let the walk be nonreversing so that it has a maximum of  $z-1$  directions to choose from for the next step. Let  $\{\mathbf{r}_j^m | m=1, 2, \dots, z_j\}$  be the unoccupied NN’s available for the  $j$ th step of the walk. If  $z_j=0$ , the walk cannot grow further because it is geometrically “trapped.” It is, therefore, discarded and a fresh walk is started from  $\mathbf{r}_0$ . If  $z_j \neq 0$ , the walk proceeds as follows:

Let  $n_{NN}^m(j)$  be the number of NBNN sites of  $\mathbf{r}_j^m$ . Then, the probability that this site is chosen for the  $j$ th step is given by

$$p_m(\mathbf{r}_j) \equiv \frac{\exp[\beta_G n_{NN}^m(j) \epsilon_0]}{\sum_{m=1}^{z_j} \exp[\beta_G n_{NN}^m(j) \epsilon_0]}, \quad (1)$$

where the summation is over all the  $z_j$  available sites. At “infinite” temperature ( $\beta_G=0$ ), the local growth probability  $p_m(\mathbf{r}_j)$  is equal to  $1/z_j$  and thus, the walk generated will be the same as the kinetic growth walk [7]. However, at finite temperatures, the walk will prefer to step into a site with more NBNN contacts. We have illustrated this local growth rule in Fig. 1(a) for IGW on a square lattice. Lower the growth temperature, less is the attrition (see the inset of Fig. 2) that the walk suffers while also being able to grow into more compact configurations. Moreover, it has been shown [6] that a  $\theta$  point for this walk exists, and that the walk belongs to the same universality class (i.e., has the same values of the universal exponents  $\nu$  and  $\gamma$ ) as the SAW above, at and below the  $\theta$  point.

\*Email address: slnoo@magnum.barc.ernet.in

†Permanent address: Materials Science Division, Indira Gandhi Centre for Atomic Research, Kalpakkam 603 012, Tamilnadu, India.

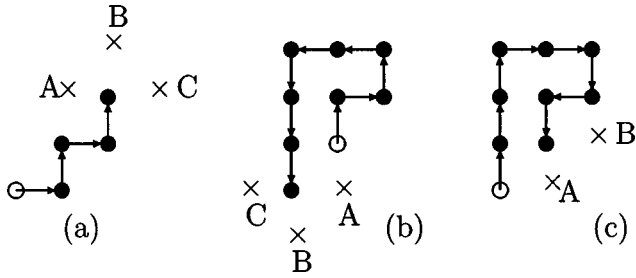


FIG. 1. A simple illustration of the IGW algorithm for generating walks from the origin, denoted by the open circle, at a given growth temperature  $\beta_G^{-1}$ . (a) The sites A, B, and C are available for making the fifth step. Choosing the site A will lead to one NBNN contact, whereas choosing the sites B or C will lead to none. Hence, the sites A, B, and C will be chosen with probabilities  $e^{\beta_G}/(2 + e^{\beta_G})$ ,  $1/(2 + e^{\beta_G})$ , and  $1/(2 + e^{\beta_G})$ , respectively. (b) The probability of growing this configuration is given by  $p_b = (1/4)(1/3)^2(1/2)^2(e^{\beta_G}/[2 + e^{\beta_G}])^2(e^{\beta_G}/[1 + e^{\beta_G}])$ . (c) The probability of growing this configuration, which is identical to (b), is given by  $p_c = (1/4)(1/3)^5(e^{2\beta_G}/[2 + e^{2\beta_G}])$ .

We have repeated the IGW simulations on a square lattice for walks up to  $N=8000$ , much longer than reported in Ref. [6] and with better statistics. In Fig. 2, we have shown the  $N$  dependence of the exponent  $\nu(N)$  obtained from the mean squared radius of gyration data, for various values of  $\beta_G$  in the range 3–10. We have estimated the asymptotic values of this exponent as simple polynomial extrapolations of these  $\nu(N)$  values, and presented them in Fig. 3, along with also those obtained for  $\beta=0, 1, 1.5$ , and 2 from the earlier data reported in Ref. [6].

The transition from the SAW phase ( $\nu=3/4$ ) to the collapsed walk phase ( $\nu=1/2$ ) seems to be taking place over a narrow range of  $\beta_G$  values ( $\sim 3.5 \leq \beta_G \leq \sim 5.0$ ), but this could still be due to limitations of our numerical work. The asymptotic estimates of  $\nu$  could improve not only with longer walks but also with larger number of successful

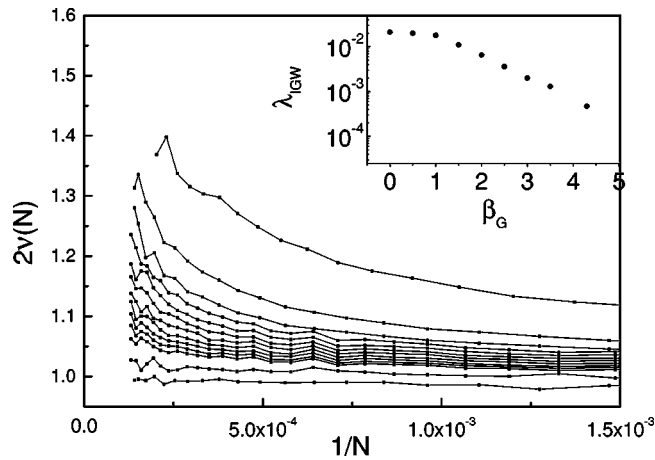


FIG. 2. The trend towards the asymptotic values of the exponent  $\nu$  for various values of  $\beta_G$  ( $=3.0, 3.5, 3.7, 3.8, 3.9, 4.0, 4.1, 4.2, 4.3, 4.4, 4.5, 5.0$ , and  $10.0$ ), from top to bottom. Inset: semilogarithmic plot of the attrition constant as a function of  $\beta_G$ . The data seem to suggest a form,  $\lambda_{IGW} \propto \exp(-a\beta_G)$ , where  $a$  is a constant.

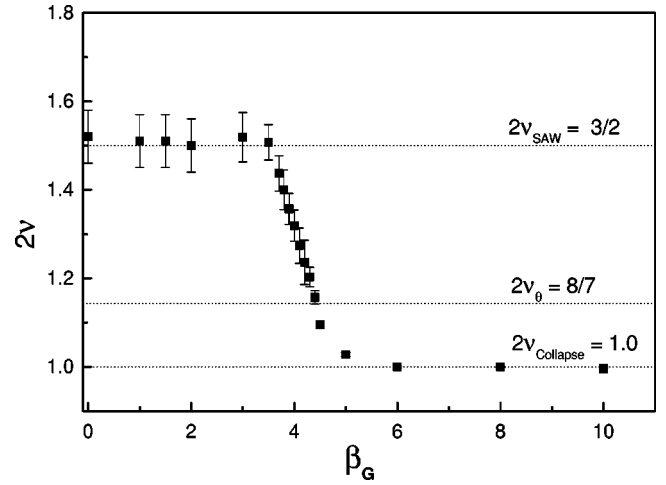


FIG. 3. The collapse scenario of IGW as brought out by the temperature dependence of  $\nu$ .

walks, and this could result in narrower transition regime. The  $\theta$  point for the IGW corresponds to a growth temperature given by  $\beta_G \sim 4.5$ , which is close to our earlier value ( $\sim 4$ ) [6]. Thus, we see that IGW has all the three distinct phases (extended,  $\theta$  point and collapsed) of SAW, realizable by tuning the growth temperature  $\beta_G^{-1}$ .

However, the IGW does not represent a homopolymer in equilibrium with its environment at some bath temperature. Because, the set of all  $N$ -step IGWs generated at a given growth temperature  $Z_{IGW}(N; \beta_G)$  is not equivalent to the canonical ensemble of ISAWs,  $Z_{ISAW}(N; \beta)$ , for some bath temperature  $\beta^{-1}$ . For example, in Figs. 1(b) and 1(c), we have shown two identical configurations which are expected to occur with the same probability in a canonical ensemble, but are in fact grown with different probabilities. This is a consequence of the fact that the local growth probability  $p_j(\mathbf{r}_j)$  of making the  $j$ th step to a site  $\mathbf{r}_j$  depends on all the previous sites visited. Hence, the probability of generating an IGW configuration,  $\mathcal{C} \equiv \{\mathbf{r}_0, \mathbf{r}_1, \dots, \mathbf{r}_j, \dots\}$ , has to be written as  $P_{IGW}(N, \mathcal{C}) = \prod_{j=1}^N p_j(\mathbf{r}_j; \mathbf{r}_0, \mathbf{r}_1, \dots, \mathbf{r}_{j-1})$ . Nonetheless, there must be a correspondence between the kinetically generated IGW and the canonical ISAW, especially because the former can be tuned to belong to the same universality classes as the latter.

Let  $\mathcal{E}_G \equiv \beta_G \epsilon_0$  denotes the dimensionless energy per NBNN contact at the growth temperature  $\beta_G^{-1}$ . Then, an  $N$ -step IGW configuration  $\mathcal{C}$  having a total of  $N_c(\mathcal{C})$  such contacts will have an energy  $E_G(\mathcal{C}) = \mathcal{E}_G N_c(\mathcal{C})$ . As illustrated in Figs. 1(b) and 1(c), configurations with the same energy are generated with different probabilities. We may rewrite the growth probability  $P_{IGW}(N, \mathcal{C})$  as follows:

$$P_{IGW}(N; \mathcal{C}) = \prod_{j=1}^N p_j(\mathbf{r}_j; \mathbf{r}_0, \mathbf{r}_1, \dots, \mathbf{r}_{j-1}) \quad (2)$$

$$\equiv e^{\mathcal{E}(\mathcal{C}) N_c(\mathcal{C})} P_{SAW}(N), \quad (3)$$

where  $P_{SAW}(N) \equiv z^{-1}(z-1)^{-(N-1)}$  is the probability of generating an  $N$ -step SAW configuration and  $\mathcal{E}(\mathcal{C})$  is the en-

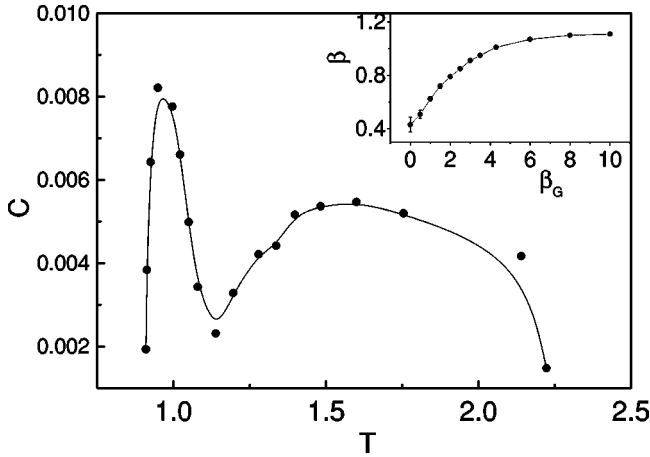


FIG. 4. Dimensionless specific heat as a function of bath temperature  $T \equiv \beta^{-1}$ . The sharp peak at  $T \sim 1$  corresponds to  $\beta_G \sim 4.5$ , and hence to the  $\theta$ -collapse transition. The continuous line is a guide to the eye. Inset: inverse of bath temperature  $\beta$  as a function of the inverse of growth temperature  $\beta_G$ .

ergy per contact to be assigned to the configuration if it were to be considered as a member of a canonical ensemble.

$$\mathcal{E}(C) \equiv \frac{1}{N_c(C)} \sum_{j=2}^N \ln[(z-1)p_j(\mathbf{r}_j; \mathbf{r}_0, \mathbf{r}_1, \dots, \mathbf{r}_{j-1})]. \quad (4)$$

It is now clear that different configurations with the same number contacts could be assigned different values of  $\mathcal{E}(C)$  because their growth probabilities are different. In other words, for a given value of the growth parameter  $\mathcal{E}_G$ , the mapping of IGW to ISAW gives rise to a distribution of the dimensionless energy per contact  $\mathcal{E}$ .

Assuming that  $\epsilon_0$  is a constant, a distribution in  $\mathcal{E}$  corresponds to a distribution in  $\beta$ . This implies that the IGW configurations grown at a given temperature  $\beta_G^{-1}$  can be considered as ISAW configurations, but sampled at temperatures drawn from a distribution in  $\beta$ . We have discussed this recently for IGW on a honeycomb lattice [8]. We have shown that a sharply peaked distribution in  $\beta$  can be associated with any given  $\beta_G > 0$  (the broadest distribution, numerically obtained for  $\beta_G = \infty$ , peaks at  $\beta \sim 1.21$  with an FWHM  $\sim 0.03$ ). In the athermal limit ( $\beta_G = 0$ ), the IGW corresponds to ISAW at a unique temperature given by  $\beta = \ln 2$ , a result obtained first by Poole *et al.* [9]. Since the distribution in  $\beta$  is sharp, the peak value may be taken to provide a well-defined canonical or “bath” temperature at which most of the IGW configurations can be considered as ISAW configurations. The ones that correspond to different temperatures will have to be equilibrated at the peak temperature.

Alternatively, if IGW were to be considered as an ISAW, then it should represent an equilibrium configuration at a uniquely defined bath temperature. We fix the bath temperature  $\beta$  by assuming that the peak position of the distribution in  $\mathcal{E}$  can be identified with  $\beta\epsilon_0$ . There is no *a priori* reason to assume that the average energy per contact for the equilibrium configuration should be the same as  $\epsilon_0$ , a parameter

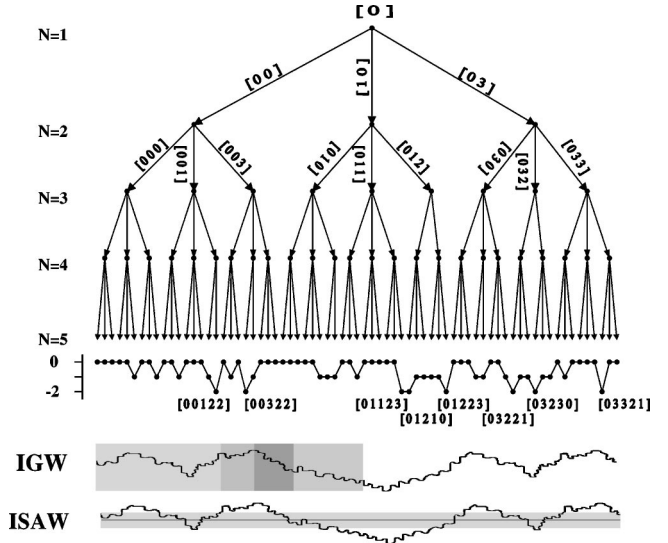


FIG. 5. A schematic illustration of how the growth of an IGW can be viewed as a hierarchical process. The configurations are coded as strings of 0's, 1's, 2's, and 3's enclosed within square brackets, where the labels 0, 1, 2, and 3 correspond to steps in the  $+x$ ,  $-y$ ,  $-x$ , and  $+y$  directions, respectively. The various paths in the hierarchy are taken with different probabilities (see text). The tree is constructed in such a way that the final configurations are numbered in increasing order from left to right. Shown just below the tree is the energy landscape for all the five-step walks whose first step is along the  $+x$  direction. Of course, the probability of realizing a point on the landscape depends on the growth temperature  $\beta_G^{-1}$ . The global minimum energy ( $= -2$ ) configurations are indicated by their respective codes. And below this is a schematic picture of the energy landscape for asymptotically long walks. In the case of IGW, the number of available (or realizable) final configurations decreases as the walk proceeds to grow. This is illustrated by shaded regions becoming progressively darker. Exactly which point on the landscape is finally reached is decided by the value of  $\beta_G^{-1}$ . In the case of ISAW, however, all the configurations having their energies within an interval (schematically indicated by the shaded region) determined by  $\beta^{-1}$  will be sampled.

introduced for sampling the locally available sites during its growth. Hence, the distribution in  $\mathcal{E}$  can be taken to be proportional to a distribution in  $\epsilon$ , peaking at  $\epsilon_0$ .

We have obtained the bath temperature  $\beta(N)$  and the width  $\sigma(N)$  of the distribution in  $\epsilon$  as a function of  $N$  for a given  $\beta_G$ , basically from the first and second moments of the distribution in  $\mathcal{E}$ . Then, we have estimated their asymptotic values by fitting them to a simple form,  $y(N) = y + (A/N^B)$ , where  $y$  ( $= \beta$  or  $\sigma$ ),  $A$ , and  $B$  are adjustable parameters. We have presented the estimated  $\beta$  values as a function of  $\beta_G$  in the inset of Fig. 4. We find that the full range of  $\beta_G \in [0, \infty]$  is mapped into a narrow range of bath temperatures,  $\beta \in [\sim 0.42, \sim 1.12]$  ( $\in [\ln 2, \sim 1.2]$ , on honeycomb lattice [8]). It may be noted that the  $\theta$  point,  $\beta_G \sim 4.5$ , corresponds to  $\beta \sim 1$ .

From the asymptotic variances  $\sigma^2(\beta)$ , we have obtained the specific heat per contact  $c(\beta) = \beta^2 \sigma^2(\beta)$ , and presented them in Fig. 4 as a function of the bath temperature  $\beta^{-1}$ . The sharp peak seen at about  $\beta \sim 1$  corresponds to the col-

lapse transition at the  $\theta$  point. This, in fact, validates the view that a definite bath temperature can be associated with the IGW.

But, there is no such known transition that can be associated with the excess specific heat seen as a broad hump above the  $\theta$  peak, because this region is in the SAW phase as far as the universal exponents are concerned (Fig. 3). It is therefore of interest to understand what is responsible for this excess specific heat. Recently, hyperquenched glasses have been shown [10] to exhibit excess specific heat (Fig. 4 of Ref. [10]), strikingly similar to what we have observed for the IGW (Fig. 4) above the  $\theta$  point. The dimensionless energy per contact  $\mathcal{E}(C)$  defined in Eq. (4), is indeed an average of such values that can be evaluated during the growth process. This implies that a distribution of  $\mathcal{E}$  can be associated with every configuration generated. Moreover, the IGW configurations are clearly much more compact (see Fig. 1 of Ref. [6]) than the typical SAWs belonging to the same universality class. It is therefore reasonable to consider them as “frozen” globules.

It may be noted that the correspondence between  $\beta_G$  and  $\beta$  whose existence is dictated by Eq. (4) forms the basis of this study. And, the fact that the full range of  $\beta_G \in [0, \infty]$  maps into a finite range of canonical  $\beta \in \sim [0.42, 1.12]$  has subtle physical implications. For example, as depicted in Fig. 5, the growth of an IGW can also be considered as a hierarchical approach towards realizing a particular configuration. Every step taken reduces the number of available configurations, or equivalently, restricts the accessible region of the energy landscape in a progressive manner. This implies that irreversible growth is equivalent to breaking the ergodicity of the system. The probability of taking a certain path in the hierarchy depends on the tuning parameter,  $\beta_G$ . On the other hand, in the canonical ensemble picture, we sample all the configurations whose energies lie within an interval defined by the bath temperature  $\beta^{-1}$  (schematically illustrated in Fig. 5). In particular, we expect to sample only those con-

figurations with global minimum energy when  $\beta^{-1}=0$ . In contrast, with  $\beta_G^{-1}=0$ , the IGW algorithm will generate a few zero energy (athermal) configurations as well, besides those with global minimum energy; hence, the corresponding  $\beta^{-1}$  will be greater than zero. And, larger the value of the coordination number  $z$  of the lattice, smaller will be the number of such athermal configurations, and hence larger will be the value of  $\beta^{-1}$  to which it corresponds. Similarly, the distribution of NN contacts for the IGW configurations generated at  $\beta_G=0$  deviates from that obtainable for SAW, and hence the corresponding  $\beta$  will be an  $z$ -dependent nonzero value.

In summary, we have shown that the IGW configurations can be considered as members of a canonical ensemble (i.e., as ISAW configurations) if the energy per contact can be considered as a random variable. In general, a meaningful statistical mechanical description of an irreversible growth process involves an element of self-generated disorder. The signature of this is seen as a broad hump in the specific heat above the  $\theta$  point. That these configurations are generated in an hierarchical manner, as implied by the specific growth rule, provides additional support to the conjecture that they may be taken to represent hyperquenched polymer configurations. Conformational dynamics of IGW could throw further light on this conjecture. In fact, the IGW seems to illustrate the generic possibility of a growth process giving rise to hyperquenched states of a system, if it is faster than the configurational relaxation.

S.L.N. is grateful to R. Chidambaram and M. Ramadham for inspiring him to study the physics of growth walks. A part of the computational work was carried out at the Institut für Festkörperforschung. K.P.N. thanks Forschungszentrum Jülich for the hospitality extended to him during March–April 2002. He also thanks V. Sridhar for fruitful discussions. We thank P. V. S. L. Kalyani for help in preparing the figures.

- 
- [1] P. G. de Gennes, *Scaling Concepts in Polymer Physics* (Cornell University Press, NY, 1979); C. Vanderzande, *Lattice Models of Polymers* (Cambridge University Press, Cambridge, 1998).
- [2] H.S. Chan and K.A. Dill, *Phys. Today* **46**, 24 (1993); V.S. Pande, A.Yu. Grosberg, and T. Tanaka, *Rev. Mod. Phys.* **72**, 259 (2000); *Protein Folding*, edited by T.E. Creighton (Freeman, NY, 1992).
- [3] V.G. Rostiashvili, G. Migliorini, and T.A. Vilgis, *Phys. Rev. E* **64**, 051112 (2001); R. Du, A.Yu. Grosberg, T. Tanaka, and M. Rubinstein, *Phys. Rev. Lett.* **84**, 2417 (2000); N.V. Dokholyan, E. Pitard, S.V. Buldyrev, and H.E. Stanley, *Phys. Rev. E* **65**, 030801(R) (2002).
- [4] H. Saluer, *J. Stat. Phys.* **45**, 419 (1986); B. Duplantier and H. Saleur, *Phys. Rev. Lett.* **59**, 539 (1987); A. Baumgartner, *J. Phys. (France)* **43**, 1407 (1982); K. Kremer, A. Baumgartner, and K. Binder, *J. Phys. A* **15**, 2879 (1982); H. Meirovitch and A. Lim, *J. Phys. Chem.* **91**, 2544 (1989).
- [5] K. Kremer and K. Binder, *Comput. Phys. Rep.* **7**, 259 (1988); A. Baumgartner and K. Binder, *Application of Monte Carlo Methods in Statistical Physics* (Springer, Berlin, 1984).
- [6] S.L. Narasimhan, P.S.R. Krishna, K.P.N. Murthy, and M. Ramadham, *Phys. Rev. E* **65**, 010801(R) (2002).
- [7] I. Majid, N. Jan, A. Coniglio, and H.E. Stanley, *Phys. Rev. Lett.* **52**, 1257 (1984).
- [8] S.L. Narasimhan, V. Sridhar, and K.P.N. Murthy, *Physica A* (to be published).
- [9] P.H. Poole, A. Coniglio, N. Jan, and H.E. Stanley, *Phys. Rev. B* **39**, 495 (1989).
- [10] V. Velikov, S. Borick, and C.A. Angell, *Science* **294**, 2335 (2001).